



Various phases in surface movements linked to deep coal longwall mining: from start-up till the period after closure

André Vervoort¹

Received: 8 January 2020 / Revised: 20 March 2020 / Accepted: 15 April 2020 / Published online: 9 May 2020
© The Author(s) 2020

Abstract This paper covers the entire lifetime of an underground coal mine, including the start-up of the mining operations and the period after the closure and sealing of the underground workings. Measurements of the vertical surface movement are presented for three neighbouring mines in the Belgian Campine coal basin, where the longwall mining method was applied. First, the monitoring of the initial phase showed that the impact of the first panel was smaller than the impacts of the following two neighbouring panels. When the second panel was mined, a change in the induced surface tilt was observed in the immediate proximity of the panels. Second, data for a transect with a length of about 2.5 km were presented, covering a total time of 54 years, of which the first 31 years were during the active life of the mine. Average subsidence rates of up to -0.3 m/year were observed. After the mine was closed and the pumping facilities were stopped, the average uplift rate was situated mostly between 4 and 16 mm/year, but a value of 141 mm/year also was measured. Thirty years after closure, the upward movements are still occurring. Third, the phase of uplift is analyzed in more detail over a full north–south transect. A clear narrow maximum was observed for the uplift, corresponding to a total vertical movement of 0.2 m over approximately an 18-year period. All these phases are relevant, for example when analysing damage to buildings and infrastructure. Damage becomes visible when the cumulative movement and loading exceed critical limits and not necessarily when the largest rate of movement is observed, for example.

Keywords Longwall · Ground control · Subsidence · Uplift · Surface movement · Radar-interferometry

1 Introduction

Subsidence linked to total extraction mining methods has been studied extensively and is still being researched. Often the studies concentrate on one aspect of the impact of mining on surface movement or they are linked to a specific problem. Most publications cover only the impacts that occur in relatively short time periods, ranging from those that occur immediately to those that occur over a period of a few months or years after mining. Sufficient data rarely are available to cover the entire lifetime of a

mine. However, damage to buildings and infrastructure becomes visible when the cumulative movement and loading exceed critical limits and not necessarily when the largest rate of movement is observed, for example. Therefore, it is important to look at all phases of surface movement.

In this paper, historical data and recent data are presented, covering the initial movement when the first panels are mined in a new area and the movements that occur several decades after the closure of the underground mine and the associated facilities. Hence, a good description of the various phases of vertical surface movements is presented. One of the reasons that data are unavailable from the start of coal mining in the European coal basins is that mining was initiated in those areas in the early years of the twentieth century or earlier. In addition, extensive multi-

✉ André Vervoort
andre.vervoort@kuleuven.be

¹ Department of Civil Engineering, KU Leuven, Leuven, Belgium

seam mining makes it more difficult to clearly identify each aspect of the surface movement. For example, when studying the impact of an individual longwall panel, the influence of earlier mined panels is still a factor. Similarly, the long-term impact of an individual longwall panel is affected by the new panels that are being mined.

When studying the impact of longwall mining on the surface, most research has focused on the vertical downward movement or subsidence. In the last two to three decades, inverse movements have been measured in European coal basins, where a large number of mines have been closed and sealed off. This uplift or vertical upward movement clearly is linked to the flooding of the closed coal mines (Baglikow 2011; Bekendam and Pöttgens 1995; Caro Cuenca et al. 2013; Samsonov et al. 2013). Upward movements also have been observed above some coal mines in Australia, but this so-called upsidence occurs during the exploitation phase and is linked to the high horizontal stresses in the strata below the valleys (Galvin 2016). Recently, the horizontal component of the surface movement is directly measured by using novel InSAR time series (Samsonov et al. 2013). Prior to this, the horizontal strain mainly was considered to be a derivative of the differential vertical movement, which forms only part of the horizontal movement. No data on the horizontal movement were available for inclusion in this paper.

Logically, it was impossible to cover all phases in this study for exactly the same locations. However, data are presented within a relatively small zone of the Campine basin in the north-eastern part of Belgium. Hence, some parameters, such as the depth of mining, the number of seams mined, the hydro-geological conditions, and others were similar for the various sets of data. The area mined in the Belgian part of the Campine basin corresponds approximately to an east–west zone with a length of about 60 km and a width of about 5–10 km in the north–south direction (Van Tongeren and Dreesen 2004; Vervoort and Declercq 2018). In other words, one can consider the mined area as a relatively narrow east–west band. Along this band, the three sets of data presented here are within an east–west distance of about 4.5 km. The data were collected above the Winterslag, Waterschei, and Zwartberg coal mines, which are neighbouring mines. There were no proper barriers between them that had not been mined. The production of coal in these three mines began in the period from 1917 to 1925. The Zwartberg mine was closed in 1966, while the two others stopped production in 1987 and 1988. The depth varied between approximately – 450 m and – 1050 m. Overall, there was a dip of 12°–16° towards the N to NNW directions. At one specific location, 5–7 different seams often were mined over the entire life of the mine, but sometimes even more seams were mined. Most of the seams had a mining height of about 1 m. The

mining method was longwall mining without backfill. Over the entire lifetime of the mines, various levels of mechanization were applied. In the first decades, individual props were used for roof support of the longwall face and the coal was excavated by hand by individual miners. Later, the coal was mined by ploughs and shearers. And in the last 25 years, the individual hydraulic props were systematically replaced by shield support along the face.

The coal seams mined in the Campine Basin in northeast Belgium belong to the Upper Carboniferous strata (Westphalian stage). The Campine Basin is part of the extensive South Permian Basin of northwestern Europe (Van Tongeren and Dreesen 2004). Above the coal strata, the overburden contains weak geological material (e.g., sand, clay and chalk) with a total thickness of 400–600 m. Several aquifers and aquitards are present over the entire section of the overburden (Vervoort and Declercq 2017). In the coal strata that is being mined, the waste rock is composed mainly of shale, siltstone, sandstone, and thin (unmined) coal layers. Overall, the successive strata are relatively thin (on the order of decimeter to meter in scale). At certain depths, massive quartz sandstone changing into orthoquartzite is recorded, but the overall thickness of this material is small. The sandstone is classed as medium-strong, with a typical uniaxial compressive strength (UCS) of 90 MPa (Caers et al. 1997). However, values up to 160 MPa have also been measured. The other types of rocks are classified as weak rock; e.g., siltstone was tested with a UCS value from 17 to 68 MPa with an average of 46 MPa, and coal with a UCS value from 6 to 10 MPa with an average of 7 MPa. The average values of Young's modulus for these three types of rocks were determined as 28 GPa for sandstone, 9 GPa for siltstone and 1 GPa for coal (Caers et al. 1997).

Three sets of data are presented. First, the focus is on the mining of three panels in the same seam in an area without any prior mining. So, we studied the initial phase of vertical surface movement or subsidence induced by the start of longwall mining. Second, data are presented along a line of about 2.5 km above an area with extensive mining. The data includes as well information on the period during the mining phase, as well as on the period afterwards, including the period after the closure and flooding of the underground infrastructure. Third, the phase of upward surface movement or uplift along a north–south transect is discussed in detail. The historical data were collected by conventional levelling techniques, but the more recent data were recorded by remote sensing. Images from the European C-band ERS1/2 and ENVISAT-ASAR satellites were used. Access to these data was obtained through a research proposal from the European Space Agency (ESA) (Devleeschouwer et al. 2008).

2 Initial impact on surface movement during the mining of three neighbouring panels

In the early 1970's, a new zone was opened up in the Winterslag mine, and a specific measuring campaign was planned to study the impact of mining three neighbouring panels on the initial subsidence. The main aim of this exercise was to determine the zone of influence or the angle of draw for the Campine basin (De Mey 1986). A straight measuring line was considered in the field, which was perpendicular to the face advance (Fig. 1). First, the panel in the middle (panel A) was mined over a period of about 1.2 years, then the panel situated more to the north (panel B) was mined, and, finally, the panel to the south (panel C) was mined. The mining of panels B and C took 1.4 years and 0.85 year, respectively. The time periods when the two panels were being mined overlapped briefly. Figure 1 shows that panel C was a short panel. Figure 2 shows the vertical surface movements at 7 points in the various graphs. The reference point is point *a*, which was situated in the middle of the width of panel A. The points at the borders of panel A are called $-b$ and *b*, and both were 110 m from the reference point. Figure 1 shows that points *c* and *d* were situated above panel C, while points *e* and *f* were farther away from the mined zone. All measurements were compared to a location at a distance of about 2.2 km along the measurement line from reference point *a*, i.e., about 1.85 km from the side of panel C (point *d*). With a

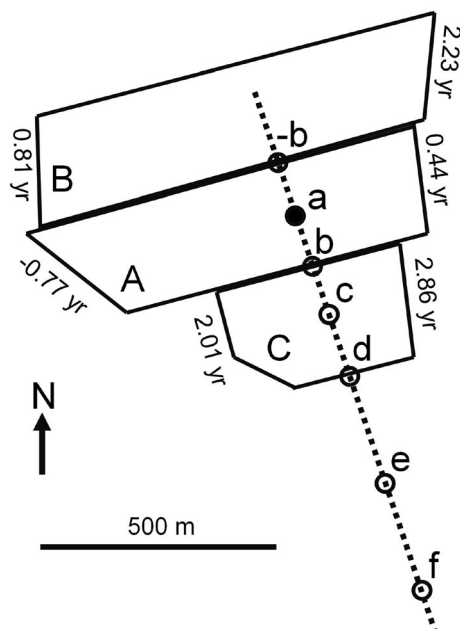


Fig. 1 Map of three neighbouring panels and measurement line with the various measurement points. Start and end of mining of each panel is indicated, using a time scale whereby the origin corresponds to the moment that the face of panel A passes underneath reference point *a*

depth of about -500 m for panel C, the latter distance is nearly 4 times the mining depth. The origin for the time was taken as the moment when the face was passing beneath reference point *a*. A Wild NA2 level instrument was used to measure accurately the movement of oak pegs or pickets driven into the ground. This instrument is known to have high accuracy, i.e., a standard deviation of 0.7 mm for 1 km. Measurements were made on an approximately monthly basis, i.e., the average time interval between measurements was 33 days.

2.1 Subsidence or vertical downward movement of the surface

Figure 2 presents information on the vertical surface movements as a function of time. Figure 2a gives an overall picture for all points over the total period of about 4 years. General conclusions are that (1) for all points, there was a systematic increasing subsidence and (2) the further away from the centre of mining the amount of subsidence decreased with the distance from the centre of mining (for example by comparing points *e* and *f* with the other points). However, by considering the data in more detail, some additional observations were formulated. First, it was interesting to note that the subsidence at the reference point *a* in the middle of the three neighbouring panels was not largest over the entire period. When mining panel A (till 0.44 year) and at the start of panel B (from 0.81 year), the subsidence at point *a* was largest in comparison to the other measuring points. However, for the time interval from 1.7 to 2.6 years, point $-b$ at the border between panels A and B represented the largest total subsidence values. At the end of the observation period, after panel C is mined (2.86 years), the reference point *a* had again undergone the largest subsidence of all points. Second, the various curves are characterised by a clear change in the rate of movement. Third, one could conclude that point *f* is at about the limit of the zone of influence for these three panels. Point *f* was 475 m from the southern side of panel C along the measuring line, so it was at a distance that was approximately the same as the depth of the longwall panel. When mining only three panels, this would mean that the angle of draw was about 45° .

Figure 2a also shows that reference point *a* had undergone a subsidence of -0.38 m at the end of mining panel A (0.44 year). Since the mining height was, on average, 1.6 m for the three panels, this subsidence value corresponds to only 24% of the mining height. Before the mining of panel B began (0.81 year), an additional movement of -47 mm had occurred over a period of 135 days, i.e., the residual rate of movement was -0.35 mm/day. When the mining of panel C began (2.01 year; panel B was not yet fully mined at that moment), reference point *a* had

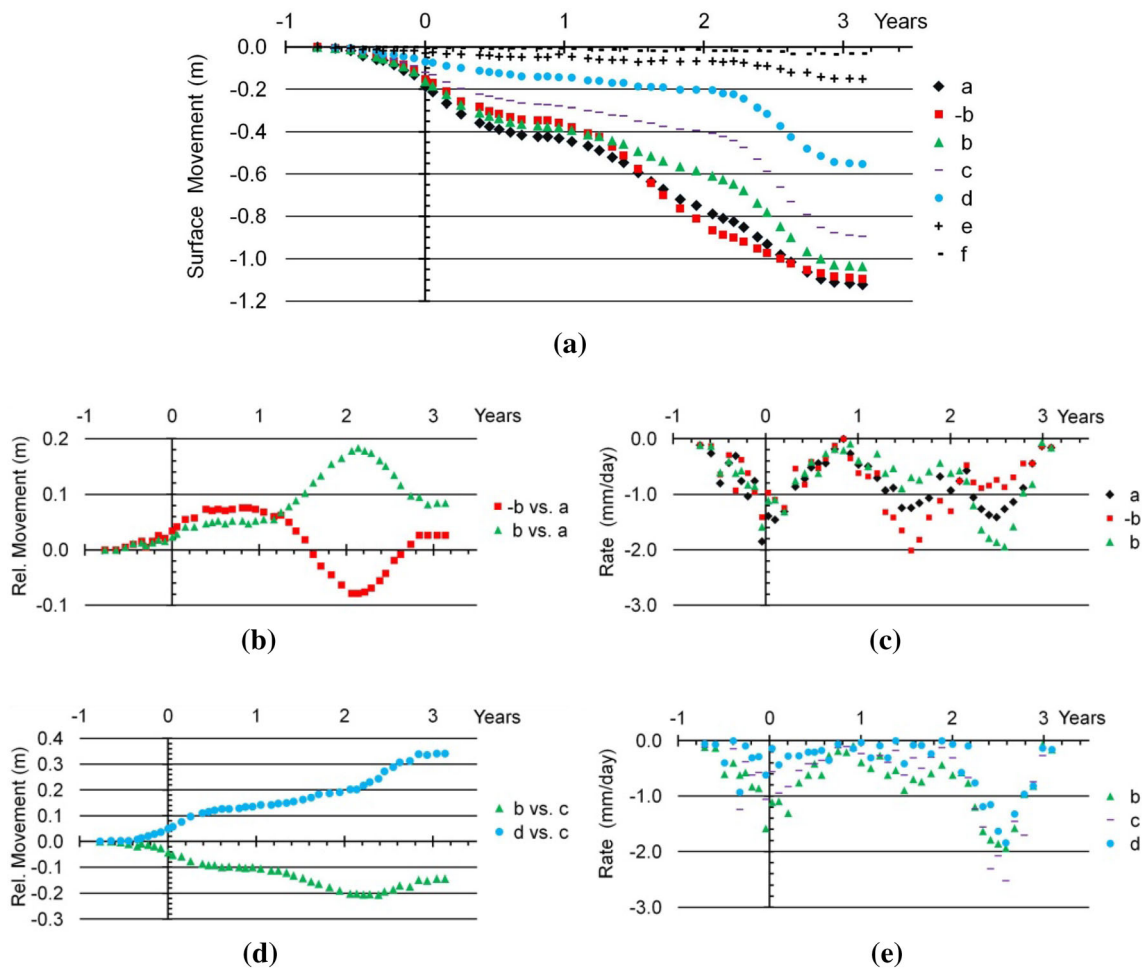


Fig. 2 Variation of subsidence as a function of time for 7 measuring points (Fig. 1) over the entire observation period of about 4 years: **a** overview graph of total vertical surface movements; **b** differences of subsidence for points $-b$ and b relative to the movement of reference point a in the middle of the width of panel A (A positive value means that the border points have undergone less subsidence.); **c** variation of the rate of movements for points $-b$, a , and b ; **d** differences of subsidence for points b and d relative to the movement of point c , situated around the middle of the width of panel C; **e** variation of the rate of movements for points b , c , and d

undergone an additional -0.37 m of vertical movement, resulting in a total subsidence of -0.79 m, which corresponded to 49% of the mining height. At the end of mining panel C (2.86 years), the total subsidence was more than a meter (-1.10 m, which was almost 70% of the mining height). In the 102 days following the end of mining panel C, the residual rate of movement was -0.25 mm/day. For a fully extended mined zone, one normally assumed that the total subsidence corresponds to 90% of the mining height in the Campine basin.

For this particular configuration and sequence of mining the three panels, the reference point situated in the middle of the central panel, which was mined first, underwent approximately the same amount of subsidence due to the mining of each individual panel. Including the residual movement, the mining of the three panels induced -0.42 m, -0.37 m (until the start of panel C), and -0.33 m, respectively. From one perspective, this is

surprising because reference point a is outside the boundaries of panels B and C. The most feasible explanation is that a minimum area had to be mined before the goaf and the fracturing of the roof layers were extended sufficiently. The thickness of the competent strata above the coal seam was about 350 m. This value is larger than the width of 220 m of panel A. However, the sum of the widths of both panels A and B was 435 m, which was slightly larger than the thickness of the competent strata. In other words, after mining two panels, and certainly after mining three panels, the affected height within the competent strata had reached the softer and weaker material. At that moment, one can assume that the competent strata layers were fractured over their entire height. Before this occurred, the non-fractured strata still partially protected the surface from the effect of the collapsed zone.

2.2 Induced tilt and rate of movement

At the end of the observation period, the three points above the middle and borders of panel A had undergone a similar total subsidence, i.e., -1.12 m, -1.10 m, and -1.04 m for points a , $-b$, and b , respectively. However, such a similar movement for these three points was not the case over the entire observation period. The mining of panel B clearly induced an asymmetric movement above panel A. In Fig. 2b, the differences of subsidence for points $-b$ and b relative to the movement of reference point a in the middle of the width of panel A are presented as a function of time. A positive value means that the border locations had undergone less subsidence. During the mining of panel A (from -0.77 year through 0.44 year), the reference point a clearly underwent the largest subsidence (-0.38 m). This is entirely logical since point a was situated above the middle of the panel that was being mined. There was a small difference between points $-b$ and b . The point to the north ($-b$) underwent 0.07 m less vertical movement, while the point to the south (b) underwent 0.05 m less vertical movement than the point in the middle (a). This could have been due to the seam's dipping to the north, but it is not certain that this is the correct explanation. The dip of the seam is about 16° in the direction of the measuring line. Once the mining of panel A was finished, the differences remained about constant until the mining of panel B began (0.81 year). Point $-b$ started to undergo more and more subsidence, and, from 1.6 years forward, it had a total subsidence larger than the reference point a . During the same period, point b underwent less subsidence than both of the other points, which is logical since this point was the farthest away (of these three points) from panel B. Around the time that panel B was mined completely and the mining of panel C had begun, the differences between points $-b$ and b reached their maximum value, i.e., 0.26 m. The differences with the middle point a were -0.08 m and 0.18 m, respectively. Over the 220 -m width of the entire panel, this resulted in an average induced tilt of 1.2 mm/m at the surface. For the southern half of the panel, the tilt averaged about 1.7 mm/m, while, for the northern half of the panel, it had an average induced tilt of 0.7 mm/m. Since the profile was not linear, larger values occurred over smaller measuring bases. However, it probably is more important that the surface tilted in different directions during the mining of these two panels. In the northern half, first, it tilted towards the south, and this was followed by a tilting to the north. This fact is important when considering the inducement of horizontal strain and the stability of buildings and other infrastructure. In the southern half, the tilt always was towards the north.

During mining panel C, the phenomena were reversed, and the total subsidence for the three points, i.e., a , $-b$,

and b , again became closer to each other. After the end of mining panel C, the relative position of the three points remained approximately constant, i.e., at 26 and 85 mm for points $-b$ and b , respectively, in comparison with reference point a . This means that the middle point (a) again had undergone the largest total subsidence. This is logical since point a is situated in the middle of the three panels.

Figure 2c shows the variation in the average rate of movement as a function of time for points $-b$, a , and b . As mentioned above, the frequency of measurements was about once a month. Hence, the average rate is expressed as mm/day. For the period that corresponds to mining panel A, the fluctuations were the largest, but, later, the curves evolved more in a systematic way, and there was a clearer distinction between the three curves. Most likely, this can be linked to the small absolute values at the start of the observation period and the larger values later on. However, it is clear that the curves of the three points present a cyclic variation with three maxima per curve (i.e., largest subsidence rate). These maxima corresponded approximately to the moments when the faces of the three panels passed the measuring line. During mining panel A, the maximum rate was for the reference point a and was recorded for 0 year for the time scale used. For mining panel B, it was for point $-b$ and at about 1.6 years, and for panel C, it was for point b at about 2.6 years. These three highest rates were approximately the same, i.e., about -2 mm/day (point a : -1.8 mm/day; point $-b$: -2.0 mm/day; point b : -1.9 mm/day). Thus, over the entire observation period of 4 years, the movement was accelerated three times and slowed down again.

Figure 2d, e show graphs similar to those in Fig. 2b, c, but Fig. 2d, e are for the points above panel C and its borders. Point c was situated around the middle of the width of panel C (i.e., at a distance of 101 m from panel A and 153 m from the other border). When comparing the movements at points b and d in comparison to the movement of the middle point c , the variation as a function of time was now different from what was observed in Fig. 2b. The surface movement of the southernmost point (point d) over the entire period was less than it was in the other two points that were considered, and, similarly, the movement of the point neighbouring panel A always was the largest of the three points considered here. In other words, the induced tilt of the surface remained to the north during the mining of the three panels, which was not the case above panel A. At the end of the observation period, the tilt over the entire width was, on average, equal to 1.9 mm/m. In comparison to point c , point b underwent an additional subsidence of -0.143 m, and point d underwent less movement of 0.341 m. When focussing on the intervals $b-c$ and $c-d$, the maximum induced tilts were 2.0 mm/m and 2.2 mm/m, respectively. These values were larger than

those above panel A. The maximum value of 2.0 mm/m in the northern half was reached at 2.38 years, after which the tilt decreased to 1.4 mm/m. The value of 2.2 mm/m in the southern half was reached at the end of the observation period.

Figure 2e shows the rate of movement of the points above and at the borders of panel C.

During mining panels A and B (until about 2 years), the rates of movement of the two different points (*c* and *d*) were significantly less than what was observed for the points above and at the borders of panel A (Fig. 2c). However, while panel C was being mined, point *c* around the middle of the panel underwent a higher rate than was observed previously. The largest average monthly rate that was recorded was -2.5 mm/day for point *c* (2.62 years). As mentioned above, the largest average rate recorded at reference point *a* was -1.8 mm/day (0 year).

3 Variation as a function of time over the entire life span of the mine, including the long-term impact

The previous paragraph focused on the initiation of the vertical movement of the surface or the subsidence when beginning to mine coal or when opening a new section of an existing mine. The measurements were frequent (about monthly) and the distances between measuring points were relatively small (from 100 to 250 m). The points were situated along a single straight line, which was relatively short, i.e., a total of 2.3 km, but movement was observed over a length of about 1 km. The total observation period was limited to about 4 years. In this paragraph, data are presented for a total observation period of 54 years. The frequency of the measurements was much less, i.e., every 5–10 years. Figure 3 shows that the length of the measuring line with movement was about 2.5 km. All measuring points for the levelling campaign were anchored at the bottom part of buildings. Hence, the roads were followed, resulting in a non-straight line. The vertical movements were measured in comparison to a reference point that was situated about 900 m more to the northeast than point A along the same road, i.e., A–B–C (De Mey 1986). These levelling data were complemented with recent remote sensing observations by satellites. Even though the frequency of the latter recordings was close to monthly, the same time interval is presented that was used for the levelling data.

As mentioned earlier, the mining took place in the Belgian Campine basin along a relatively narrow east–west band over a length of several 10's of km with a limited north–south width. While the previous case was situated at the southern part of the mined zone, the measuring line

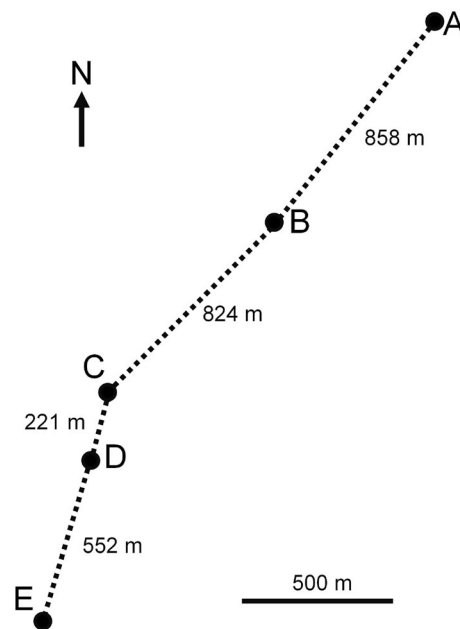


Fig. 3 Map of the measurement line with the various measurement points

discussed here is in the northern part. The east–west distance between both cases was about 1 km. The mining took place approximately south of point B (Fig. 3). Table 1 provides information concerning the mining that occurred below and in the immediate vicinity of each measuring point. It must be pointed out that mining did not occur in the entire area of each seam that was mentioned, but at least one longwall panel was mined in the immediate vicinity of the measuring point (within a range of 500 m). The nine seams that were mined at point E represented a total mining height of 11.2 m. More to the north than point E, the number of seams mined decreased, but the total height of the mining still was 6.8 m close to point B, and it covered 6 seams. The period of mining is given in comparison to the start of the measurements. No mining had occurred prior to that moment, except for one small panel

Table 1 Number of seams mined below and in the immediate vicinity of each measuring point and some additional information (i.e., total mining height, depth range, and period of mining)

Measuring point	Number of seams mined	Total mining height (m)	Depth interval (m)	Period of mining (years)
A	–	–	–	–
B	6	6.8	– 636...– 956	4–22
C	7	7.7	– 557...– 947	0–27
D	8	9.1	– 557...– 947	0–27
E	9	11.2	– 497...– 800	0–22

11 years earlier close to point *E*. The depth interval increased to the north, which is logical since the dip of the strata was towards the N to NNW direction. The mine was closed in year 31 on the time scale that was used. Hence, the movement was recorded for about 23 years after the closure.

3.1 Total vertical movement of the surface

Figure 4 shows the variation of the vertical movement of the surface as a function of time for the five measuring points over the entire observation period of 54 years. It is immediately clear that the sizes of the movements for most points were on the meter scale. A few years after the mine was closed (in year 31), the surface started to move upwards. The total additional upward movement was on the order of the decimetre scale until the last measurement for year 54. For most points, the maximum subsidence was recorded for 35.5 years. For all observations, and in particular to determine the maximum values, one should realize that the frequency of measurements in time and space was relatively low. In other words, the real maximum could have been reached some time earlier or later and its value could have been larger.

Point *A* underwent a small amount of movement, which means that the choice of the reference point of about 900 m more to the northeast than point *A* was a good choice. However, even though the movement was small, it is interesting to note that the maximum subsidence was

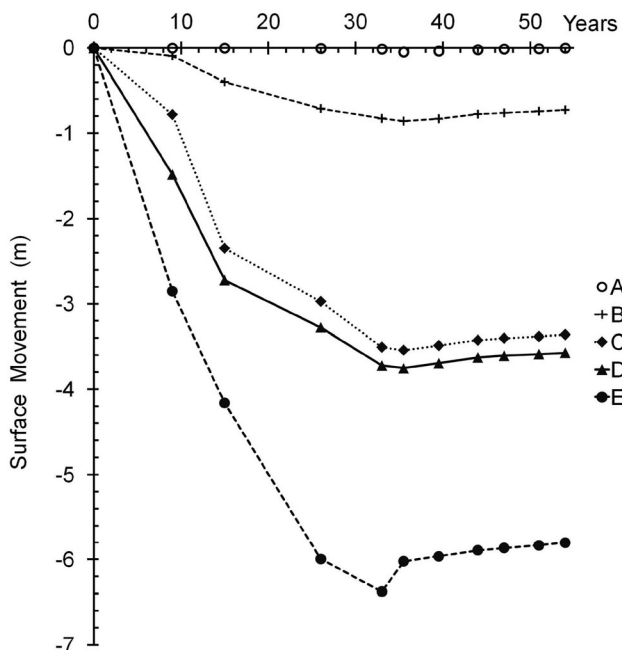


Fig. 4 Variation of surface movement as a function of time for 5 different measuring points over the entire observation period

reached at 35.5 years. At that time, this point had undergone a subsidence of -45 mm in comparison to the reference point. The last measurement (year 54) at point *A* showed that the full amount of subsidence had been compensated by uplift. So, for point *A*, an uplift of 45 mm was recorded from year 35.5 through year 54. Point *A*, towards the north, was situated about 700 m from the most northern longwall panel in this area. Since there is no indication that the uplift has stopped, the total cumulative movement became positive after year 54 at point *A*.

The most southern measuring point (*E*) logically underwent the largest subsidence because that is where most of the mining took place. The maximum subsidence of -6.38 m was reached in year 33. However, afterwards, the surface moved upwards until year 54 over a vertical distance of 0.58 m. All other points reached their maximum subsidence by year 35.5, but we must consider the remark made earlier about the moment of maximum and its link with the measuring frequency. The maximum subsidence values recorded for points *B*, *C*, and *D* were -0.86 m, -3.54 m, and -3.75 m, respectively. The amounts of uplift for *B*, *C*, and *D* for the period of 18.5 years (from year 35.5 through year 54) were 132 mm, 182 mm, and 180 mm, respectively. Although it could be said in general terms that the larger the subsidence is, the larger the upward movement will be, this is not the case when looking in detail at individual measuring points (Bekendam and Pöttgens 1995; Vervoort 2020). The ratio between uplift and maximum subsidence is not fixed. In addition to this observation, it also is a problem that, for both phenomena, the final subsidence or uplift is unknown, since both processes do not reach equilibrium until many decades have passed. By comparing the uplift at year 54 to the maximum subsidence recorded (for year 33 or 35.5), a ratio is calculated equal to 15.4%, 5.1%, 4.8%, and 9.0%, respectively for points *B*, *C*, *D*, and *E*. For point *A*, outside the undermined area, both movements are similar.

3.2 Induced tilt

Considering the tilt that was induced during the subsidence and uplift phases, the maximum value was 2.7 mm/m based on the average over the straight distance between the two extreme points, i.e., points *A* and *E*. Over the first 9 years of observation, it was 1.2 mm/m and it increased until year 33. After year 33, it decreased slightly to a value of 2.4 mm/m. For the successive pairs of points, the maximum tilt was observed between points *D* and *E*, i.e., there was an induced tilt of 4.9 mm/m for year 26. The second largest average induced tilt was observed between points *B* and *C*, i.e., 3.3 mm/m for years 33 and 35.5. During the uplift phase, it remained approximately constant (final value of 3.2 mm/m for year 54). The induced tilt

between points *C* and *D* reached its maximum value of 3.2 mm/m in year 9. Subsequently, it decreased systematically to 1.0 mm/m. The induced tilt between points *A* and *B* reached its maximum value, i.e., 1.0 mm/m, for years 33–35.5. Afterwards, it decreased to 0.8 mm/m. All of the tilts presented here were towards the south. However, a decrease in total tilt (since the start of the measurements and of the movement) means that, between two observation moments, the additional induced tilt was to the north. For example between points *C* and *D*, a tilt of 2.3 mm/m to the north was induced from year 9 through year 44. For points *D* and *E*, an additional induced tilt of 0.9 mm/m to the north was observed after year 26. A similar observation was made for the first case, where it clearly was observed that the additional tilt as well as the total tilt changed directions. However, it must be remembered that both the distance between the successive measuring points and the time interval between measurements were larger in the second case. Hence, there is a reasonable likelihood that a change in the total tilt direction could not be detected.

3.3 Rate of movement

Table 2 presents the average rates of vertical movement between the successive measuring moments for the 5 points that were monitored. These data only provide some

information on the order of magnitude of the rate because the time intervals were relatively large. So, larger rates certainly have occurred within a given time interval. The rates of vertical movement around the change subsidence-uplift also must be interpreted critically. Either the last negative rate or the first positive rate is the average of subsidence and uplift. Table 2 also provides the number of longwall panels that were mined in the vicinity of each measuring point during each interval. This figure is different from the number of seams mined in Table 1 because more than one panel could be mined within a given seam. When 4–5 panels were mined in the immediate vicinity (as shown by the green colour) in a particular time interval, the average subsidence rates were determined to be in the range of – 87 to – 261 mm/year. For the first time interval of 9 years, 8 panels were mined in the vicinity of point *E* (purple colour), and this resulted in an average subsidence rate of – 0.3 m/year. For the time intervals with 1–3 mined panels (yellow colour), the average rates varied between – 10 and – 77 mm/year. Residual average rates of subsidence of – 13 to – 55 mm/year were recorded for the time intervals without any mining in the immediate vicinity of points *B*, *C*, *D*, and *E* (grey colour) and after the closure of the mine (year 31). Since these are the last intervals with subsidence, the real residual subsidence rates most likely were larger.

Table 2 Average rates (mm/year) of vertical surface movement between the successive measuring moments for the 5 points that were monitored

Point	Period (years)									
	0-9	9-15	15-26	26-33	33-35.5	35.5-39.5	39.5-44	44-47	47-51	51-54
A	0.0 (-)	0.0 (-)	-0.3 (-)	-1.3 (-)	-13.4	2.4	3.1	2.8	1.6	2.2
B	-10.4 (2)	-50.5 (2)	-28.6 (3)	-16.1 (0)	-13.0	6.5	12.2	5.3	4.4	5.8
C	-86.8 (5)	-261.2 (4)	-56.6 (1)	-76.7 (1)	-13.6	13.6	14.0	7.1	5.4	7.2
D	-165.0 (5)	-206.2 (5)	-50.5 (1)	-63.4 (1)	-12.5	14.5	15.0	7.2	4.1	5.4
E	-316.9 (8)	-218.3 (5)	-166.5 (4)	-54.7 (0)	141.12	14.9	16.0	9.2	8.0	10.6

A negative value means downward movement, and a positive value means upward movement. The number of longwall panels per time period mined in the neighbourhood of each point is mentioned between the brackets

The largest average uplift rate recorded was 141 mm/year (Point *E*). Overall, the uplift rates were, on average, between 4 and 16 mm/year.

4 Upward surface movement above and around the entire mined area after the closure of the mine

In this paragraph, the emphasis is solely on the phase that corresponds to the upward movements of the surface. No data were available on the movements prior to the closure of the coal mines within the zone that was analysed. Figure 5 shows the uplift over two 5-year periods along a north–south transect. Limiting the observations to two 5-year periods facilitates the comparison. As mentioned earlier, the area that was mined in the Belgian Campine coal basin is a relatively narrow band that is orientated in the east–west direction with a total length of about 60 km. The north–south width varies between 5 and 10 km. Hence the variation is larger in the north–south direction than in the east–west direction. The number of available reflectors was the main criterion for selecting a transect. The one that

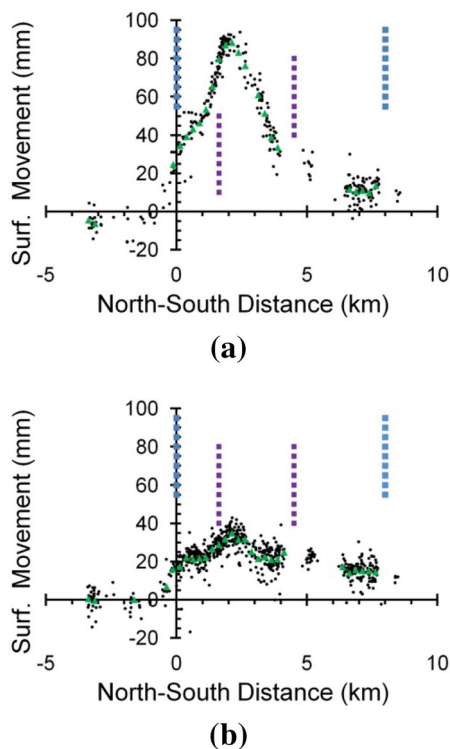


Fig. 5 Upward surface movements (each individual measurement and averages, when more than 5 reflectors are detected in an interval of 250 m) along a north–south transect measured during two 5-year periods: **a** June 1995–June 2000; **b** August 2005–August 2010. Limits of mined area in north (right) and south (left) are indicated in blue dotted lines, and borders between concessions are indicated in purple

was chosen was close to the two previous study areas, i.e., about 3 km farther to the west than the previous measurement line. Figure 5a represents the 5-year period between June 1995 and June 2000, during which measurements were recorded by the European C-band ERS1/2 satellite. Figure 5b covers the data from the ENVISAT-ASAR satellite for the 5-year period from August 2005 to August 2010. The first period was situated at the end of the full satellite observation period, so that the probability of still observing subsidence was very small. The second period also was at the end, so that the difference in the upward movements of the surface was the largest between the two figures. Figure 6 shows that the new transect was situated above the Winterslag coal mine (most southern concession), the Waterschei coal mine (in the middle), and the Zwartberg coal mine (to the north). The Zwartberg mine was closed in 1966 and the underground was sealed



Fig. 6 Map of the mined panels below and around the central transect line, indicated by the black double arrow. The total north–south distance of the mined area is 8 km. The average positions of the five locations are presented along the central line (same colour code as Fig. 8; location α is situated at a distance of -3.125 km). Concession lines between the three coal mines are indicated in purple (south and west: Winterslag mine; middle: Waterschei mine; north: Zwartberg mine)

off, so all pumping was stopped in that mine. After the closure, there was an overflow into the other two operating mines, but it was mainly into the underground of the Winterslag mine. The transect considered was above the most eastern panels in the Zwartberg mine. In Fig. 6, the map shows that there were no real barriers between the three mines. Sometimes, even the mining in the three mines overlapped when different seams were being mined. The total length of the mined area along this transect was 8 km. The southern-most point of mining was selected as origin of the north–south distance. The two borders between the three concessions were situated at distances of 1.625 km and 4.5 km along the transect.

4.1 Shape of the uplift curve along a north–south transect

One of the disadvantages of the satellite data is that the satellite has to detect reflectors, which mainly are the roofs of buildings. Hence, no recordings are made over agricultural land, semi-natural land, or forests. This means that there were gaps in the measurements where no reflectors are detected along the total length of 15 km presented in Fig. 5. This was especially of concern to the north of the mined zones for the Campine basin. Hence, it was not possible to study accurately the extent of the zone of influence to the north of the mined zone. Figure 5a is based on the data acquired from 324 reflectors, while Fig. 5b is based on the data acquired from 666 reflectors. When more than 5 reflectors are detected within an interval of 250 m, an average is calculated and presented as a green triangle in Fig. 5.

In examining the data for the first period, the most striking conclusion was that a very clear maximum was observed in the curve. The maximum average was situated at a distance of 2.125 km, and it reached a value of 88.3 mm over 5 years, so the average annual rate was about 18 mm/yr. More to the south and to the north, the uplift decreased sharply. For example, at distances of 1 km to the south and 1 km to the north of the maximum, the average uplifts were 53.6 and 61.0 mm, respectively. Thus, the additional movement represented a change in tilt of 3.5 and 2.7 mm per 100 m, respectively. At the southern limit of the mining (distance of 0 km), the upward movement was about 30 mm over the 5-year period. Over the interval between the southern limit and the maximum, there could be a bent in the curve. However, small subsidence values were recorded about 3 km to the south. (See also further.) Although there were two gaps in the measurements available above the Zwartberg mine, it still could be concluded that the upward movement was significantly less than it was in the other two mines. The average values were about 10 mm for the zone between 6.5 and 8 km. In earlier

studies in the Campine basin, it often was observed that the shape of the uplift curves corresponded well to a symmetrical inverse trough shape (Vervoort 2016; Vervoort and Declercq 2018). For the transect studied here, the shape was not symmetrical over the entire length of past mining. As mentioned above (Fig. 6), the transect that was considered was in the northern part at the limit of the most eastern panels in the Zwartberg mine.

The data for the second 5-year period showed an interesting observation (Fig. 5b), i.e., the additional vertical movement above the most recently closed mines had decreased significantly, while this was not the case above the Zwartberg mine that was closed in 1966. The maximum still was situated around 2.125 km, but an additional average movement of 35.0 mm was observed, corresponding to a rate of 7 mm/yr, which was much smaller than the rate observed in the first period (18 mm/year). At 1 km more to the north and to the south, the additional movement was about 22 mm. Thus, the shape of the curve was much flatter than it was in the first period. The additional change in tilt was now only 1.3 mm per 100 m. Around a distance of 7 km, the uplift was about 15 mm in the second 5-year period that was considered, and this uplift was slightly larger than that in the first period. At least, these observations show that the phenomenon of upward movement is complex and that time has an important impact.

4.2 Information on mining

Figure 7 gives more details of the longwall panels underneath the central transect line for successive intervals of 250 m. Figure 7a shows that there was overall an increase of the mining depth towards the north. Around the southern border, the mining depths were between -500 and -550 m, while the deepest panel was at a depth of -1000 m for a distance of 3.375 km. The mining was the most extensive between distances of 0.75 km and 3.5 km. The total height of the mining varied from 7 to 9 m, representing 5–7 panels mined above each other at different times. The Zwartberg mine was the first of the 7 mines to be closed in the Belgian Campine basin (1966), but the mining in this mine occurred along the central transect between 1964 and 1966. So, not long before closure. In the other two mines, the mining started along the transect much earlier, i.e., in 1930 or shortly thereafter. The last panel mined along this transect was in 1972. For the zone between the distances of 0.75 and 3.5 km, where mining was the most extensive, the mining was done over many years. However, between a distance of 1.25 and 2.5 km, no panels were mined after 1959. Overall, most panels along this transect already had been mined when the Zwartberg

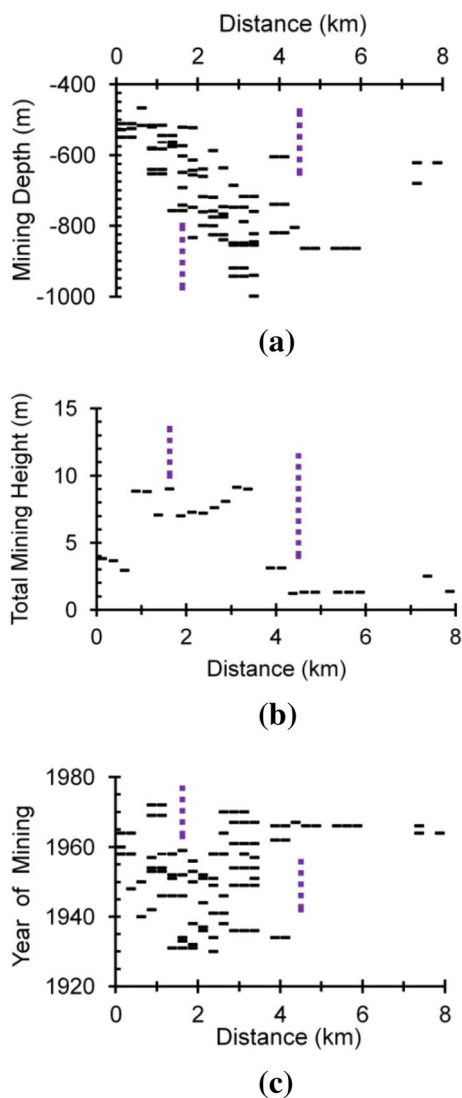


Fig. 7 Details of the longwall panels just underneath the central transect line: **a** average mining depth of each individual longwall panel; **b** total mining height of all longwalls; **c** year of mining of the individual longwall panels

coal mine was closed in 1966. Only 11 of 90 panels were mined after 1966.

Although the maximum uplift (i.e., at a distance of 2.125 km) occurred within the zone of extensive mining, i.e., between 0.75 and 3.5 km, there was no real correlation between the amount of mining and the uplift directly above the mining. If there had been some correlation, the maximum uplift would have occurred around 1 or 3.25 km, or a constant value of uplift between 0.75 and 3.5 km would have been observed. The observation was in agreement with earlier studies. In Vervoort (2020), a detailed study was presented that compared the values of residual subsidence and uplift. For the western part of the Campine coal basin, the satellite data also covered the period of residual subsidence. Although the average rates of residual

subsidence and uplift are of the same order of magnitude in absolute terms, the spatial distributions of the residual subsidence values and the uplift values are different. No correlation was observed between these two parameters. However, one can assume that there would be a good correlation between subsidence (and, thus, also residual subsidence) and the characteristics of the mined longwall panels. In other studies of the Campine basin, no correlation was found between the latter characteristics and the recorded uplift values (Vervoort 2016; Vervoort and Declercq 2018).

4.3 Increase of uplift as a function of time

Figure 8 shows the variation of uplift as a function of time for 5 distances along the transect line. (See the map in Fig. 6.) The 10 reflectors that were closest to the chosen north–south distances were selected, and an average was calculated. The first point (α) was situated outside the mined area, at a distance of -3.125 km to the south, and the last point (ϵ) was situated at a distance of 6.875 km above the Zwartberg mine. The middle point (γ) was situated close to the maxima in the curves presented in Fig. 5, i.e., at a distance of 2.125 km. Finally, the two remaining points were situated at distances of 1.75 km to the south (β) and 1.5 km to the north (δ) of point γ , respectively. The total period was slightly more than 18 years, and it included an interpolated period of 3 years between both datasets. In Fig. 8, the two 5-year periods of Fig. 5 are indicated by arrows.

The upward movement at or close to the overall maximum increased systematically as a function of time (Fig. 8a), and it reached a total movement of 218.5 mm after about 18 years of observation. The rate of movement decreased as time passed, which also was observed in Fig. 5. Figure 8a shows the averages for 10 reflectors as well as the maximum and minimum values. For a given observation period or type of satellite, the 10 reflectors were always the same. However, they could be different for different observation periods. As can be seen, the fluctuation was relatively limited. Between two successive observation moments, the maximum fluctuation was between 3 and 5 mm. On average, the range between the two extreme measurements was about 25 mm, with a minimum of 10 mm and a maximum of 40 mm. This variation is only partly linked to measurement errors and inaccuracy. It also is affected by the spatial distribution of the 10 reflectors that were selected. The range for each set of satellite data was relatively constant as a function of time, which indicates that the method is accurate.

Figure 8b shows the variation of points β and δ . Only the averages are presented, but the range from the minimum to the maximum was similar, as shown in Fig. 8a.

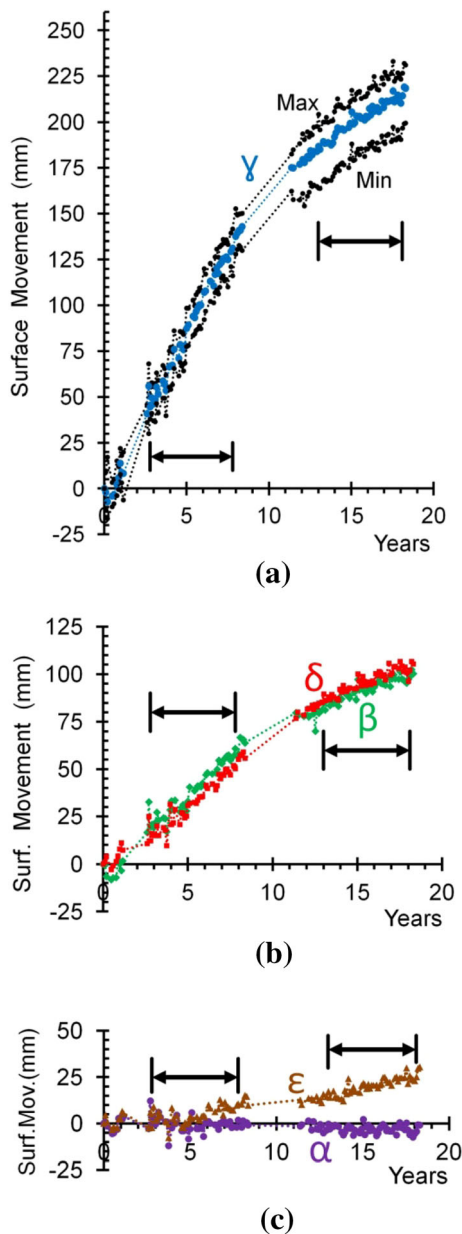


Fig. 8 Variation of the upward surface movement as a function of time from mid-August 1992 to mid-October 2010, based on remote sensing data (The average is presented for the 10 reflectors closest to the five N–S distances): **a** location γ , at a distance of 2.125 km (minimum, average, and maximum values are presented); **b** locations β and δ , at distances of 0.375 and 3.625 km, respectively; **c** locations α and ϵ , at distances of -3.125 and 6.875 km, respectively. The two 5-year periods of Fig. 5 are indicated by arrows

The same observations can be made that were made for point γ . The average values of β and δ after 18 years were 100.3 and 105.4 mm, respectively. Over the 18-year period, this resulted in an average additional change in tilt of 1.8 mm/100 m to the south of the maximum value at point γ and 1.5 mm/100 m to the north.

Although Fig. 5a would lead one to assume that there was still some subsidence south of the southern mining limit, this is not confirmed in Fig. 8c (point α). Over the 18 years of observation, the average was close to zero, and no trend was visible. However, point ϵ underwent a slow, but systematic, increase of upward movement and reached 30.6 mm after 18 years. Often, the accuracy of the rate of movement is assumed to be about 1 mm/year for an individual reflector (Marinkovic et al. 2009; Agioutantis et al. 2019). This is slightly smaller than the rate observed for the average movement around point ϵ . Since the increase in Fig. 8c (point ϵ) is systematic, one can consider it to be significant or trustworthy.

5 Discussion of findings

Surface movement induced by a total extraction method with caving, such as longwall mining with goaf, most likely is one of the more complex problems in the field of rock mechanics and ground control. The emphases in most research and monitoring projects are on the vertical movement of the surface and the impact within a relatively short period. First, the reason for the focus on the vertical surface movement is that this component is the largest in almost all cases. Also, it is the easiest component to measure by conventional levelling techniques. Galvin (2016) gave some examples of measuring horizontal displacements. Hu and Lian (2015) and Luo (2015) also specifically modelled the horizontal displacements. Recently, some research has also been done in Europe on the horizontal component of the movement by using the novel InSAR time series (Samsonov et al. 2013). By studying the vertical movement of the surface, one of the relevant questions to be answered is the extent of the zone of influence, e.g., the angle of draw (Cai et al. 2016). The latter clearly is different from one coal basin to another, and it is influenced by the geological conditions (Peng 1986; Wagner and Schümann 1991; Galvin 2016; Chugh 2018). Second, one of the reasons that most research focuses on either the immediate impact of longwall mining or the impact over a period of a few years is that most research addresses a specific problem or question. Another reason clearly is that, generally, long-term research projects seldom are done. Hejmanowski (2015) looked specifically at a time interval of 25 years. The work by Al Heib et al. (2005) and Gueguen et al. (2008) focused on the residual subsidence, but limited it as a function of time.

In the paper, data over the entire lifetime of a mine, including the period after closure, are presented and studied. Due to the availability of remote sensing data, it has become easier to study the surface movement over long time periods and after the closures of mines. The latter is a

period in which mining companies often are less interested and, therefore, dedicate limited resources to such studies. In the various European coal basins, a period of residual subsidence, followed by a long period of uplift after the flooding of the underground workings, can be detected by the satellite data (Baglikow 2011; Bekendam and Pöttgens 1995; Caro Cuenca et al. 2013; Samsonov et al. 2013). Our main aim in this paper was to present data associated with the various phases of surface movement, ranging from the start of mining to the period after closure. All of the data that have been presented were recorded within a relatively small part of the Belgian Campine coal basin. The main advantage of this approach is that the various cases can be compared, although it has been shown that large variations can occur over small distances (Vervoort and Declercq 2017). Of course, the disadvantage is that the results are only fully representative of a particular area.

In the paper, the rate of movement and the induced tilt were calculated for the various cases and phases. The information on the rates is summarized in Table 3, and the induced tilts are presented in Table 4. For both parameters, one should be aware that the values presented are only indicative values. The values of the various parameters are influenced significantly by the time and distance intervals between the measurements. The averages are smoothed for the larger intervals. By considering shorter intervals, the spread of the values would become larger, and, thus, the real maximum rate or tilt also would be larger than the values presented in Tables 3 and 4. Earlier research showed that the rate of residual subsidence, averaged over about an 8-year period, varied from -2.8 to -8.7 mm/year in a particular area of about 2 km^2 , with an average over all reflectors of -5.5 mm/year, while the largest annual increase in 1 year was -30 mm (Vervoort and Declercq 2017). Something similar was valid for the uplift phase. The average rate over a period of almost 7 years was 8.6 mm/year, but it varied between 1.5 and 12.4 mm/year for different reflectors. Again, when considering the rate over a particular year, the variation was still larger, and the maximum rate was 32 mm/year. Hence, since the length of the interval is so important, this information also is included in Tables 3 and 4.

Table 3 clearly confirms that the subsidence rate was the largest during mining, which is logical. (See the data for Cases I and II.) However, the vertical movement of the surface is a sequence of accelerations and decelerations. Various concepts are used in literature when authors are dealing with residual subsidence. Some authors consider it to be the period after the direct impact of the mining (Al Heib et al. 2005; Gueguen et al. 2008). That also is the definition used for Case I in Table 3. However, a long-term residual subsidence also occurs. Residual subsidence has been observed as long as 40–60 years after mining in a

Table 3 Overview of the rates of vertical surface movement for the various datasets discussed in the paper

Case I: Phase of initial impact	Case II: Entire life of mine	Case III: Phase of uplift
Subsidence during mining panel(s), above middle of panel: maximum values of -1.8 to -2.5 mm/day (Time interval: 30 days)	Over entire subsidence phase: maximum value of -0.53 mm/day (Time interval: 33 years) Over entire uplift phase: maximum value of 0.08 mm/day (Time interval: 21 years)	Over entire observation period: maximum value of 0.03 mm/day (Time interval: 18 years)
Residual subsidence, directly after mining above panels: average values of -0.25 to -0.35 mm/day (Time interval: 100 to 135 days)	Subsidence between successive measurements (above mined area): average values of -0.03 to -0.87 mm/day (Time interval: 6 to 11 years)	Over 5-year periods: maximum value of 0.05 mm/day (start) and 0.02 mm/day (end) (Time interval: 5 years)
	Subsidence between successive measurements (above mined area): average values of -0.03 to -0.87 mm/day (Time interval: 6 to 11 years)	
	Uplift between successive measurements (above mined area): average values of 0.01 to 0.39 mm/day (Time interval: 3 to 4.5 years)	

Information is provided for the time between measurements

certain area (Vervoort and Declercq 2017). One can even wonder whether the full strata will ever reach full equilibrium or, maybe more realistically, whether it will take 100 years or more to reach that equilibrium. For the Campine basin, the direction of movement has been inverted, and upward vertical surface movement or uplift has been observed several years after the closure of the underground facilities. In other areas of the Campine basin, the absolute rates in the residual subsidence phase and in the uplift phases were of the same order of magnitude (Vervoort 2016). For example, an average rate of uplift of 9 mm/year was observed for a 5-year period in one of the western coal mines, but the average rate of subsidence of -6 mm/year in the 5 years following the closure. For

Table 4 Overview of the induced tilt by the vertical movement of the surface for the various datasets discussed in the paper

Item	Time interval	Distance
<i>Case I: Phase of initial impact</i>		
Induced tilt during mining phase		
Maximum values of 1.7–2.2 mm/m	1–3.5 years	100–150 m
<i>Case II: Entire life of mine</i>		
Over maximum distance of movement		
Maximum value of 2.7 mm/m	33 years	2300 m
Between neighboring points		
Maximum value of 4.9 mm/m	26 years	552 m
Change in tilt direction		
Maximum value of 2.3 mm/m	35 years	221 m
<i>Case III: Phase of uplift</i>		
Induced tilt during uplift		
Maximum values of 0.03 mm/m	5 years	1000 m

Information is provided on the distance and time between measurements

Case III, uplift rates of 0.02–0.05 mm/day were measured, corresponding to an annual uplift of approximately 5–20 mm, respectively. This seems small, but it should be remembered that large total uplift values are reached as the uplift continues. In another area of the Campine basin, a total uplift of 0.5 m was observed at the end of 2010, and the area is still moving upwards (Vervoort 2020).

The average values of tilt in Table 4 are affected heavily by the distance between two neighbouring measuring points and the time interval between two measurements. These effects probably even exceed the effect on the rate. The most interesting observations are for Case I, in which the distance is 100–150 m (half the width of the longwall panels). As discussed earlier, one could observe a change in the direction of the tilt between the mining of successive panels. If measurements had been made over shorter distances between points, probably even more could have been learned about the variation of tilt in space and over time. For Case II, the tilt values that were obtained were consistent with what one would expect during the subsidence phase (Al Heib et al. 2005). The main problem with the data of Case III is that the tilt induced before the uplift phase was not recorded.

6 Conclusions

The aim of the paper is not to discuss the impact (short- and long-term) of mining, through surface movements, on infrastructure and buildings. It is logical, however, that

subsidence of metre-scale had a significant impact. In certain areas in the Campine basin, such amounts of subsidence led to permanent flooding of the surface if the water were not to be pumped out permanently. The subsidence also caused visible damage to buildings and infrastructure. However, there was also a weakening of the buildings, e.g., by inducing micro-cracks. The impact of the relatively smaller upward movement should not be underestimated, especially since the older buildings have already suffered the impact of the subsidence. As explained above, the spatial distribution of the subsidence versus the uplift is different (Vervoort 2020). This means that the uplift is not a simple rebound of part of the past subsidence. Therefore, the impact should not be underestimated of the differential movements and torsions, linked to the uplift and applied to the already damaged or weakened buildings. In other words, one should never focus on one phase only, but a complete picture of the different phases is useful and necessary. This was the main aim of the paper. Even if the impact of the surface movement is not discussed in this paper, at least one should be aware that visible damage not necessarily only occurs in the period with the largest amount or the largest rate of movement, or with the largest differential movement. All phases and the entire history are relevant.

Funding There were no external sources of funding for conducting this research.

Compliance with ethical standards

Conflict of interest The authors declare that there is no conflict of interest.

Availability of data and materials At this moment the raw data have not been released to be open to the public.

Consent for publication Not applicable.

Ethics approval and consent to participate Not applicable.

Open Access This article is licensed under a Creative Commons Attribution 4.0 International License, which permits use, sharing, adaptation, distribution and reproduction in any medium or format, as long as you give appropriate credit to the original author(s) and the source, provide a link to the Creative Commons licence, and indicate if changes were made. The images or other third party material in this article are included in the article's Creative Commons licence, unless indicated otherwise in a credit line to the material. If material is not included in the article's Creative Commons licence and your intended use is not permitted by statutory regulation or exceeds the permitted use, you will need to obtain permission directly from the copyright holder. To view a copy of this licence, visit <http://creativecommons.org/licenses/by/4.0/>.

References

- Agioutantis Z, Robertson J, Gollaher G, Schaefer N, Silva J, Tripolitsiotis A, Partsinevelos P (2019) Permanent scatterer radar interferometry as an effective structure deformation monitoring tool over undermined areas. In: Proceedings of the SPIE 11174, 7th international conference on remote sensing and geoinformation of the environment. <https://doi.org/10.1117/12.2533713>
- Al Heib M, Nicolas M, Noirel JF, Wojtkowiak F (2005) Residual subsidence analysis after the end of coalmine work. In: Example from Lorraine colliery, France. Proceedings of the symposium post mining 2005, Nancy
- Baglikow V (2011) Schadensrelevante Auswirkungen des Grubenwasseranstiegs—Erkenntnisse aus dem Erkelenzer Steinkohlenrevier. *Markscheidewesen* 118(2):10–16
- Bekendam RF, Pöttgens JJ (1995) Ground movements over the coal mines of southern Limburg, The Netherlands, and their relation to rising mine waters. In: Proceedings 5th international symposium on land subsidence, The Hague, The Netherlands, IAHS 234, pp 3–12
- Caers J, Swennen R, Vervoort A (1997) Petrography and X-ray computerized tomography applied as an integral part of a rock mechanical investigation of discontinuities. *Trans Inst Min Metall Sect B Appl Earth Sci* 106:B38–B45
- Cai Y, Jiang Y, Liu B, Djamaluddin I (2016) Computational implementation of a GIS developed tool for prediction of dynamic ground movement and deformation due to underground extraction sequence. *Int J Coal Sci Technol* 3:379. <https://doi.org/10.1007/s40789-016-0151-0>
- Caro Cuenca M, Hooper AJ, Hanssen RF (2013) Surface deformation induced by water influx in the abandoned coal mines in Limburg, The Netherlands observed by satellite radar interferometry. *J Appl Geophys* 88:1–11. <https://doi.org/10.1016/j.jappgeo.2012.10.003>
- Chugh YP (2018) Concurrent mining and reclamation for underground coal mining subsidence impacts in China. *Int J Coal Sci Technol* 5:18. <https://doi.org/10.1007/s40789-018-0189-2>
- De Mey K (1986) Subsidence in the Campine basin. MSc thesis to obtain degree of Mining Engineer, KU Leuven, Leuven
- Devleeschouwer X, Declercq PY, Flamion B, Brixko J, Timmermans A, Vanneste J (2008) Uplift revealed by radar interferometry around Liège (Belgium): A relation with rising mining groundwater. In: Proceedings of the symposium post-Mining 2008, Nancy
- Galvin JM (2016) Ground engineering—principles and practices for underground coal mining. Springer, Berlin
- Gueguen Y, Al Heib M, Deffontaines B, Fruneau B, de Michele M, Raucoules D, Guise Y (2008) The interferometry technics applied on residual subsidence analysis measurement of closure coal mines, example from Nord-Pas-de Calais coal mine, France. In: Proceedings of the symposium post-mining 2008, Nancy
- Hejmanowski R (2015) Modeling of time dependent subsidence for coal and ore deposits. *Int J Coal Sci Technol* 2:287. <https://doi.org/10.1007/s40789-015-0092-z>
- Hu H, Lian X (2015) Subsidence rules of underground coal mines for different soil layer thickness: Lu'an Coal Base as an example, China. *Int J Coal Sci Technol* 2:178. <https://doi.org/10.1007/s40789-015-0088-8>
- Luo Y (2015) An improved influence function method for predicting subsidence caused by longwall mining operations in inclined coal seams. *Int J Coal Sci Technol* 2(3):163–169. <https://doi.org/10.1007/s40789-015-0086-x>
- Marinkovic P, Ketelaar G, van Leijen F, Hanssen RF (2009) INSAR quality control: analysis of five years of corner reflector time series. In: Proceedings of the Fringe 2009 workshop, Frascati
- Peng S (1986) Coal mine ground control, 2nd edn. Wiley, Hoboken
- Samsonov S, d'Oreye N, Smets B (2013) Ground deformation associated with post-mining activity at the French–German border revealed by novel InSAR time series method. *Int J Appl Earth Obser Geoinform* 23:142–154. <https://doi.org/10.1016/j.jag.2012.12.008>
- Van Tongeren P, Dreesen R (2004) Residual space volumes in abandoned coal mines of the Belgian Campine basin and possibilities for use. *Geol Belg* 7(3-4):157–164
- Vervoort A (2016) Surface movement above an underground coal longwall mine after closure. *Nat Hazards Earth Syst Sci* 16:2107–2121. <https://doi.org/10.5194/nhess-16-2107-2016>
- Vervoort A (2020) Long-term impact of coal mining on surface movement: residual subsidence versus uplift. *Min Rep Glückauf* 156(2):136–141
- Vervoort A, Declercq PY (2017) Surface movement above old coal longwalls after mine closure. *Int J Min Sci Technol* 27(3):481–490. <https://doi.org/10.1016/j.ijmst.2017.03.007>
- Vervoort A, Declercq PY (2018) Upward surface movement above deep coal mines after closure and flooding of underground workings. *Int J Min Sci Technol* 28:53–59. <https://doi.org/10.1016/j.ijmst.2017.11.008>
- Wagner H, Schumann EHR (1991) Surface effects of total coal-seam extraction by underground mining methods. *J SAImm* 91(7):221–231